ISSN 2075-1133, Inorganic Materials: Applied Research, 2021, Vol. 12, No. 2, pp. 491–498. © Pleiades Publishing, Ltd., 2021.
Russian Text © The Author(s), 2020, published in Perspektivnye Materialy, 2020, No. 11, pp. 34–44.

GENERAL PURPOSE MATERIALS

Peculiarities of the Formation of High-Coercivity Structure of (Sm, Zr)(Co, Cu,Fe)$_z$ Alloys in Varying the (4*f*-,4*d*-)-to-(3*d*-) Element Ratio

N. A. Dormidontov[a], *, N. B. Kolchugina[a], Yu. V. Milov[a], and A. G. Dormidontov[a]

[a] *Magnetoelectromechanics LLC, Moscow, 123458 Russia*

**e-mail: ontip@mail.ru*

Received August 10, 2020; revised September 12, 2020; accepted September 13, 2020

Abstract—Processes of the formation of the high-coercivity state of the $Sm_{0.85}Zr_{0.15}(C0_{0.702}Cu_{0.088}Fe_{0.210})_z$ alloys with different indices $z = 6.0$, 6.5, and 6.8, which characterize the (4*f*-,4*d*-)-to-(3*d*-) element ratio, are studied. Correlations between the chemical composition of samples and their microstructure and the coercive force, which is formed in the course of isothermal aging and aging during slow cooling (or stepped annealing), are shown. The interrelation between the high-coercivity state and quantitative relationship (volume fractions) of the main structural components based on the 2:17R and 1:5H phases is discussed. The cellular morphology of the alloy, which corresponds to the high-coercivity state, is shown to form during isothermal aging, whereas the final phase compositions of the main structural components form in a temperature range from the isothermal aging temperature to 400°C upon stepped (slow) cooling or quenching. The magnetic properties of samples in the high-coercivity state are determined by the completeness of phase transformations in the main structural components, which substantially depends on their quantitative relations and the (4*f*-,4*d*-)-to-(3*d*-) element ratio.

Keywords: Sm–Co alloys, coercive force, phase transformations, heat treatment, high-coercivity state

DOI: 10.1134/S2075113321020118

INTRODUCTION

The problem of the formation of the high-coercivity state in the (Sm, Zr)(Co, Cu, Fe)$_z$ alloys for permanent magnets continues to remain in the focus of attention of investigators owing to the fact that the knowledge about the phase transformations occurring in the course of precipitation hardening of the alloys is incomplete.

As for the structural state formed after supersaturated solid-solution heat treatment, a consensus is likely to be reached. The supersaturated solid solution with the disordered hexagonal $TbCu_7$-type structure (space group *P*6/*mmm*) is likely to be the main phase component of the alloys subjected to high-temperature homogenizing annealing at 1150–1180°C and quenching. In the course of subsequent isothermal and stepped aging, the solid solution transforms with the formation of a cellular structure [1–8].

In general, contradictions related to the structure of the (Sm, Zr)(Co, Cu, Fe)$_z$ alloy subjected to the complete cycle of heat treatments also are resolved. The optimum structure of the alloy in the high-coercivity state contains cells in the form of hexagonal bipyramids, the height of which is arranged along the easy-magnetization axis of the alloy; they are distributed discretely with a period of 60 to 200 nm in accordance with the composition and heat treatment of the alloy and are formed by rhombohedral Th_2Zn_{17}-type phase (space group $R\bar{3}m$). The cells are separated by continuous network of a phase that is coherent with the cell structure, has the hexagonal $CaCu_5$-type structure (space group *P*6/*mmm*), and forms the boundary between the cells, which is 6–20 nm in thickness (boundary phase). The whole anisotropic cell–boundary body is penetrated by thin elongated *Z*-phase plates (lamellas) 2–4 nm thick, which, in turn, are coherent to the cellular and boundary phases. As for the structure of lamellas, there are disagreements in the literature. According to data of [3, 4], they are the hexagonal Th_2Ni_{17}-type phase (space group $P6_3/mmc$); however, according to recent studies, the prevailing view is that the structure of the *Z* phase is rhombohedral of Be_3Nb-type (space group $R\bar{3}m$) [1, 7].

The cellular phase is depleted of Sm, Zr, and Cu and enriched in Fe with respect to the integral composition of the alloy. The boundary phase is enriched in Sm and Cu and is characterized by low Fe and Zr contents. The lamellar phase is the main acceptor of zirconium [1–8].

The considered structure ensures the efficient coercive-force mechanism upon magnetization reversal, namely, the domain wall pinning at the interface between cells and boundary phase. Such a coercivity mechanism is due to high gradients of the main magnetic constants in passing from a cell to a cell through a boundary. This mechanism is confirmed by magnetization curves, major and minor hysteresis loops, corresponding calculating micromagnetic models, and direct observation of domain walls of real samples of (Sm, Zr)(Co, Cu, Fe)$_z$-based magnets in using Lorentz microscopy [1–8].

That concludes the common view about the formation of high-coercivity structure. There are two models of phase transformations occurring in the course of isothermal and stepped aging of the (Sm, Zr)(Co, Cu, Fe)$_z$ alloys.

The first model assumes the decomposition of solid solution, which is accompanied by direct formation of final phases corresponding to the high-coercivity state in the course of isothermal aging [1–4, 8]. Supporters of this model assume that, during stepped aging (or slow cooling), no phase transformations occur; only element exchange or redistribution of elements between phases takes place, which is due to the temperature dependences of the solubility of these elements in the formed phases.

The second model assumes the presence of additional phases, which belong to the (Sm, Zr)$_{n-1}$(Co, Cu, Fe)$_{5n-1}$ homologous row and are present as consumed structural components. These phases form at the boundary between cells in the course of isothermal aging; the 1:5H phase forms at the boundary structural component in the course of stepped (or slow) cooling owing to element exchange in accordance with the variable solubility curves and occupies the entire volume between cells. Thus, the final high-coercivity structure of the alloy forms, which, as in the case of the first model, consists of the 2:17R + 1:5H + Z phases [5–7, 9].

When the first model of phase transformations is taken, it is impossible to explain the paradoxical difference in the values of the coercive force of samples which were quenched after isothermal aging and subjected to the complete cycle of heat treatments for the high-coercivity state, namely, isothermal aging and aging upon slow cooling from the isothermal aging temperature to 400°C (stepped aging), and of samples in the high-coercivity state which were subjected to complete aging cycle and heated to the isothermal aging temperature for several minutes and quenched to room temperature. Their coercive force and, therefore, the structural state return to those corresponding to the end of isothermal aging; this is the "return" phenomenon. The ultimate coercive force of samples can be restored only by repeated stepped aging (or slow cooling) of them [1, 2, 7–9].

In contrast, when we take the second model, according to which the intermediate consumed (Sm, Zr)$_{n-1}$(Co, Cu, Fe)$_{5n-1}$ phases are participating, the "return" phenomenon or the restoration of the properties and structure are logically explained by the existence of phase transformations in the temperature range between the isothermal aging temperature and that of the end of stepped aging.

Peculiarities of the magnetic hardening of sintered (Sm, Zr)(Co, Cu, Fe)$_z$ magnets in varying the integral chemical composition of the starting alloy argue in favor of the second mechanism of phase transformations.

In particular, it was noted in [7] that the coercive force (H_{cj}) of sintered Sm$(Co_{0.67}Cu_{0.07}Fe_{0.22}Zr_{0.04})_{7.4}$ (which corresponds to $(Sm_{0.77}Zr_{0.23})(Co_{0.70}Cu_{0.07}Fe_{0.23})_{5.48}$) magnets which were heat treated after isothermal aging (800°C for 16 h) without the stepped aging does not exceed 1 kOe; this is related to the composition of boundaries between cells formed by alternating layers of 2:7 and 5:19 phases [6, 7]. In contrast, the same samples subjected to complete aging (aging at 800°C for 16 h + cooling to 400°C at a rate of 1°C/min), the boundary phase of which was transformed into the 1:5H phase, exhibit the coercive force H_{cj} = 31 kOe [7].

The similar dependence of the coercive force was demonstrated for the sintered samples characterized by very different ratio of 3*d* elements [1]; the Sm$(Co_{0.784}Fe_{0.100}Zr_{0.028})_{7.19}$ composition (corresponding to $(Sm_{0.83}Zr_{0.17})(Co_{0.81}Cu_{0.09}Fe_{0.10})_{5.82}$) exhibits the coercive force H_{cj} = 1.4 kOe without slow cooling and H_{cj} = 25.6 kOe after complete aging under close time–temperature conditions. Despite the obtained results, specialists of the scientific school from the National Institute for Materials Science (Tsukuba, Japan) are supporters of first variant of phase transformations in the (Sm, Zr)(Co, Cu, Fe)$_z$-based magnets [1, 2].

The sintered $Sm_{0.84}Zr_{0.16}(Co_{0.70}Cu_{0.07}Fe_{0.23})$-based samples studied by us exhibit qualitatively different dynamics of magnetic hardening [10]. After aging under the same conditions (800°C for 16 h) and quenching, the coercive force was found to be higher by an order of magnitude and is H_{cj} = 15.6 kOe; the complex aging accompanied by slow cooling (800°C for 16 h + cooling to 400°C at a rate of 1.5°C/min) leads to the increase in H_{cj} to 30 kOe. In our opinion, such a result is caused by structural peculiarities, namely, by quantitative proportions of main structural components, which are related to the (4*f*-,4*d*-)-to-(3*d*-) element ratio in the integral chemical composition of the alloy [10].

The analogous behavior of the sintered Sm$(Co_{0.65}Fe_{0.26}Cu_{0.07}Zr_{0.02})$-based magnets (the composition of which corresponds to $Sm_{0.87}Zr_{0.13}(Co_{0.66}Cu_{0.07}Fe_{0.25})_{6.6}$) was noted in [9]. The samples subjected to aging at 830°C for 10 h and quenching exhibit the coercive force H_{cj} = 8.65 kOe;

after complete aging, it is 31.5 kOe. The second variant of phase transformations in the (Sm, Zr)(Co, Cu, Fe)$_z$ alloys was confirmed on the basis of X-ray diffraction and electron diffraction data, which showed changes in the phase composition of samples during isothermal aging at 830°C for 0.5–20 h. Throughout the time of isothermal annealing, the main structural components were found to be the 2:7R and 5:19H boundary phases and the 2:17R cellular phase [9]. According to [9], the noted behavior of the coercive force exclusively is related to a peculiarity of the starting alloy, namely, to the chemical composition that is markedly enriched in iron with respect to that of traditional alloys of this type.

The aim of the present study is to investigate the features of the formation of the high-coercivity state of precipitation-hardened (Sm, Zr)(Co, Cu, Fe)$_z$ alloys for permanent magnets upon varying the (4*f*-,4*d*-)-to-(3*d*-) element ratio in their chemical composition, which determines the volume fractions of the main structural components in the magnetically hard alloy.

The study was performed using samples prepared from individual grains of coarse-grained ingots of experimental alloys characterized by completely collinear components of phase structure.

EXPERIMENTAL

The $Sm_{0.85}Zr_{0.15}(Co_{0.702}Cu_{0.088}Fe_{0.210})_z$ alloys with $z = 6.0$, 6.5, and 6.8 were prepared by high-frequency induction melting of individual components using Al_2O_3 crucibles; the melting was performed in a high-purity argon atmosphere at a pressure in the operating chamber exceeding the atmospheric pressure by 5–10%. The following starting components were used: Sm >99.9%, Zr >99.97%, Co >99.98%, Fe >99.7%, and Cu >99.97%. After melting of all components and mixing, the melt was slowly cooled in the crucible that was thermally isolated from a water-cooled inductor. As a result, an ingot characterized by coarse grains 4–6 mm in average size was obtained. The ingots were crushed to individual grains. The magnetic state of each grain was characterized only by the single easy magnetization axis (EMA). These grains cannot be called single crystals in the classic sense of this term since they are not single-phase. However, all phases composing a grain are collinear; in other words, EMAs of each phase within the grain are parallel to each other. From here on, these grains and samples prepared from them are called pseudo-single crystals.

The solid-solution treatment of selected grains was performed at 1150–1180°C for 5 h and followed by water quenching. The isothermal aging at 800°C was conducted for 4, 8, 12, 16, and 20 h and either was finished by water quenching or continued by stepped aging upon cooling to 400°C at an average rate of 90 K/h and, after that, furnace cooling. Before all heat treatments, the samples were subjected to degassing by heating to 600°C in a vacuum; after that, the chamber was filled with high-purity argon to a pressure slightly exceeding (by 5–10%) the atmospheric pressure.

Pseudo-single-crystal samples subjected to different heat treatments were ground to form perfect spheres 2.5–3.5 mm in diameter using a special abrasive tool. The magnetic properties of samples were measured at room temperature in fields of ±30 kOe using a VSM Model 9600 (LDJ Electronics Inc.) vibrating-sample magnetometer, which was calibrated with a Ni standard (the specific saturation magnetization of nickel is $\sigma_{sNi} = 54.4$ (G cm^3)/g).

The samples with characterized magnetic parameters were demagnetized with an alternating field with decreasing amplitude, mounted in mandrels, and fixed with a polymeric compound. The fixation was performed using a special tool and a magnetic field in order that the prismatic plane of sample was aligned parallel to the plane of the prepared section. Sections were prepared in accordance with standard methods using diamond pastes.

To reveal the microstructure, etched microsections of samples were studied with optical magnifications (using a Neophot 32 optical microscope). Quantitative relations of structural components were determined using standard stereometric metallographic methods.

The chemical composition of solidified alloys was studied by inductively coupled plasma optical emission spectrometry (using an ULTIMA 2 Jobin-yvon ICP-OES spectrometer). The correspondence of studied samples to the integral composition of alloys was checked by electron microprobe analysis of microsections using an EPMA-SEM Camebax installation and pure metals as the standards; the maximum microsection surface was scanned.

RESULTS

In accordance with the obtained data on the integral composition of experimental alloys and actual samples, their compositions correspond to the formula $Sm_{0.85}Zr_{0.15}(Co_{0.72}Cu_{0.088}Fe_{0.210})$, where $z = 6.03$, 6.51, and 6.79 (hereinafter, z = 6.0, 6.5, and 6.8, respectively).

Figure 1 shows dependences of the coercive force of pseudo-single-crystal samples on the time of isothermal aging at 800°C. The results are given for two variants of final heat treatment, namely, for subsequent quenching to room temperature (curves *1a–3a*) and aging during slow cooling to 400°C (curves *1b–3b*).

As the typical magnetization reversal portions of major hysteresis loops of the experimental samples, Fig. 2 shows the series of dependences for the samples subjected to isothermal treatment for 16 h. Figure 2a shows the dependences for the samples quenched to room temperature directly after isothermal holding. Figure 2b shows the dependences for the pseudo-sin-

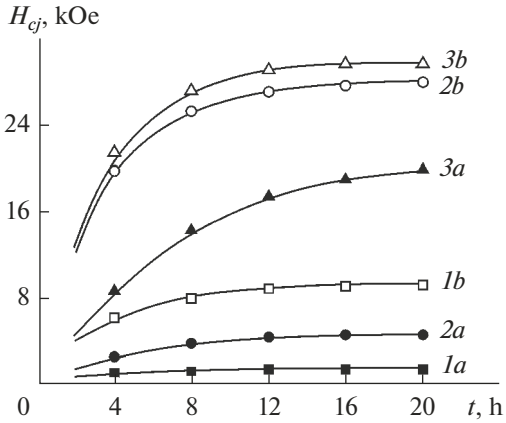

Fig. 1. Effect of time of isothermal aging at 800°C followed by either (*1a–3a*) quenching to room temperature or (*1b–3b*) slow cooling to 400°C on the coercive force of $Sm_{0.85}Zr_{0.15}(Co_{0.702}Cu_{0.088}Fe_{0.210})_z$ samples with different z: (*1*) 6.0, (*2*) 6.5, and (*3*) 6.8.

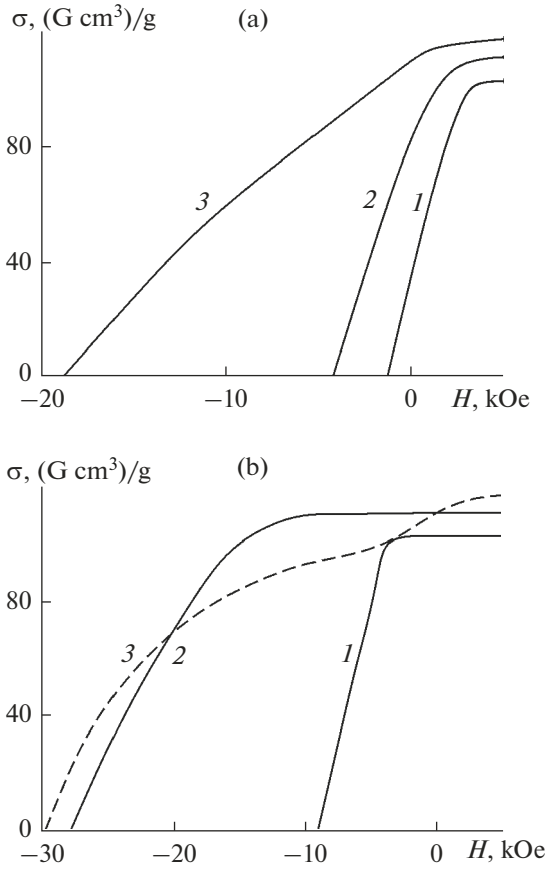

Fig. 2. Magnetization reversal portions of major hysteresis loops of experimental $Sm_{0.85}Zr_{0.15}(Co_{0.702}Cu_{0.088}Fe_{0.210})_z$ samples with z = (*1*) 6.0, (*2*) 6.5, and (*3*) 6.8 subjected to isothermal aging at 800°C for 16 h and subsequent either (a) quenching to room temperature or (b) slow cooling to 400°C; vibrating-sample magnetometer, without taking into account the demagnetizing factor, $N = 1/3$.

gle-crystal samples subjected to subsequent slow cooling to 400°C.

Figure 3 shows the microstructure (taken with optical magnification) on the prismatic plane of the $Sm_{0.85}Zr_{0.15}(Co_{0.702}Cu_{0.088}Fe_{0.210})_z$ samples with z equal to (a) 6.0, (b) 6.5, and (c) 6.8.

The shown microstructures correspond to samples in the high-coercivity state, namely, samples subjected to isothermal aging at 800°C for 16 h and subsequent slow cooling to 400°C. However, it is known that the quantitative ratios of volume fractions of the main structural components A, B, and C (based on the 1:5, 2:17, and 2:7 phases, respectively) are unchanged in the course of heat treatment, from the moment of solidification [10–12]; only the contrast and brightness of hues of structural components change slightly.

Figure 3 demonstrates monotonic variations of the volume fractions of structural components in samples upon varying the (4*f*-,4*d*-)-to-(3*d*-) element ratio, i.e., the value of z for the (Sm, Zr)(Co, Cu, Fe)$_z$ alloys.

Figure 4a shows the relationships of volume fractions of structural components A, B, and C for the series of $Sm_{0.85}Zr_{0.15}(Co_{0.702}Cu_{0.088}Fe_{0.210})_z$ alloys. The corresponding dependences of the coercive force of samples these alloys subjected to isothermal aging at 800°C for 16 h and subsequent quenching are shown in Fig. 4b (curve *1*); the dependence for the sample subjected to the complete cycle of heat treatments for the high-coercivity state is given in Fig. 4b (curve *2*).

DISCUSSION

The microstructure of cast magnetically uniaxial (Sm, Zr)(Co, Cu, Fe)$_z$-based samples, which was taken with optical magnifications, is characterized by the presence of three structural components A, B, and C (Fig. 3) based on the 1:5, 2:17, and 2:7 phases, respectively [10–12].

Structural component C is present in the form of narrow lamellar precipitates arranged along the basal plane of the anisotropic structural body; the volume fraction of the component is 0.02–0.07. As z increases, the volume fraction of the component monotonically decreases (Fig. 4a).

The sum of volume fractions of structural components A and B, which occupy the entire volume of alloy, is 0.93–0.98; these volume fractions mainly determine the hysteretic properties of samples.

In terms of the concentration range of this experimental series, the volume fraction of structural component B monotonically increases from zero to ~0.65 at the expense of a proportional decrease in the volume fraction of component A (Fig. 4a). In the most high-coercivity structural state of samples, i.e., after isothermal and stepped aging, the increase in the volume fraction of component B is accompanied by an

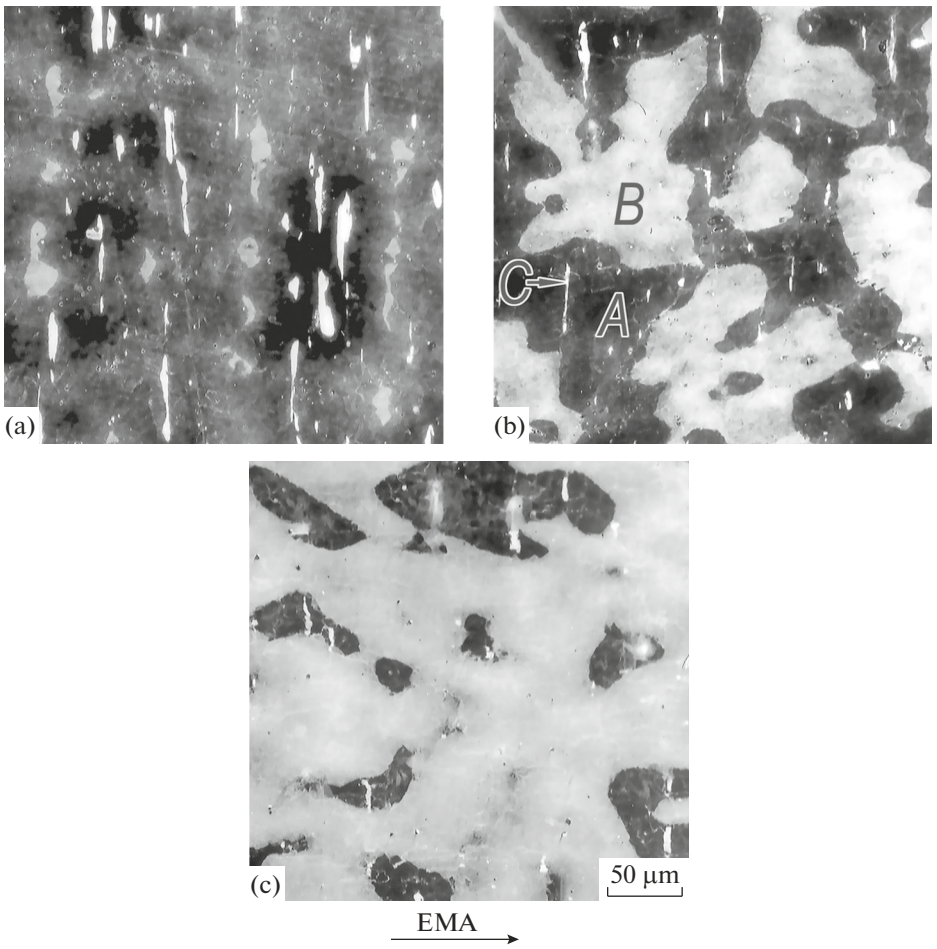

Fig. 3. Microstructure on the prismatic plane of pseudo-single-crystal $Sm_{0.85}Zr_{0.15}(Co_{0.702}Cu_{0.088}Fe_{0.210})_z$ samples with z = (a) 6.0, (b) 6.5, and (c) 6.8 in the high-coercivity state after complete cycle of heat treatment; optical microscope, etching in 5% alcoholic solution of HNO_3. EMA is the easy magnetization axis for all reported samples.

intense increase in the coercive force H_{cj} until the equality of volume fractions $V_A = V_B$ occurs. After that, the increase in H_{cj} stops, and the dependence $H_{cj} = f(z)$ goes to a plateau (Fig. 4b, curve *2*).

All alloys corresponding to the condition $V_A \geq V_B$ exhibit almost ultimate hysteresis loops. The magnetization reversal curves of the samples are characterized by not only the implementation of equality $4\pi J_S = B_R$ but also the correctness of expression $(BH)_{max} = (4\pi J_S)^{2/4}$ (Fig. 2b, curves *1* and *2*).

However, when the condition $V_A < V_B$ occurs, the squareness of the hysteresis loop worsens, and a "bending" appears in the magnetization reversal portion of the loop; the value of "bending" increases as the difference $(V_B - V_A)$ increases (Fig. 2b, curve *3*).

The dynamics of magnetic hardening in using the quenching preceded by isothermal aging is strictly centrally symmetrical (Fig. 1, curves *a* and Fig. 4b). To a first approximation, the "plateau" in the dependence $H_{cj} = f(z)$ takes place at $V_A > V_B$, and low values of the coercive force occur; the intense increase in the coercive force is observed in a composition range of alloys characterized by a dominating volume fraction of structural component B ($V_A < V_B$).

It is known [11, 12] that the fine phase structure corresponding to areas of structural component B is identical to the cellular structure of sintered (Sm, Zr)(Co, Cu, Fe)$_z$ magnets. In the high-coercivity state, the domain structure of component B and processes of the domain structure transformation in applied magnetic fields repeat the domain structure and its behavior for magnets sintered from fine powders. Upon magnetization reversal, it is characterized by reverse domains formed from numerous centers. In this case, only domains of submicron width develop, which grow only along the maximum size. As the external field increases, the section area is filled with reverse domains by means of added new domains and increase in the amount of domain walls rather than by increase in the domain width.

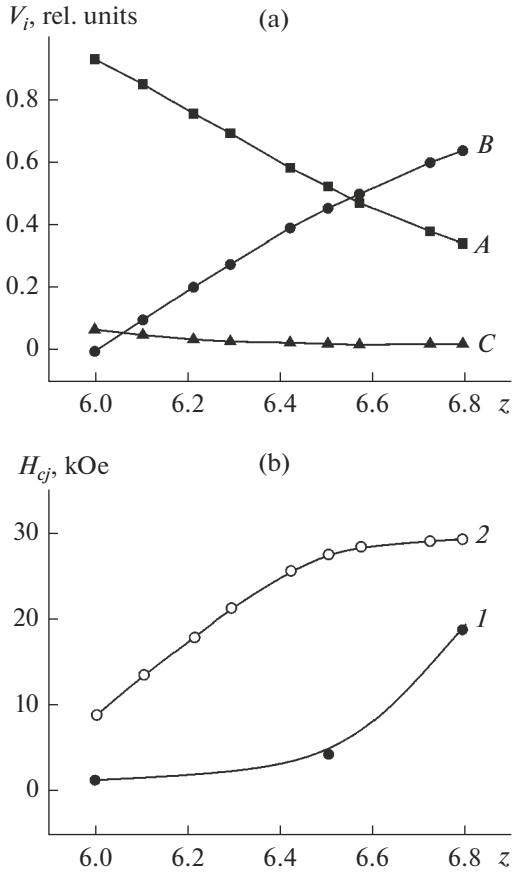

Fig. 4. Dependences of (a) volume fractions of structural components A, B, and C (V*i*) and (b) coercive force (H_{cj}) on the (4*f*-,4*d*-)-to-(3*d*-) element ratio (z) for the $Sm_{0.85}Zr_{0.15}(Co_{0.702}Cu_{0.088}Fe_{0.210})_z$ alloys subjected to isothermal aging at 800°C for 16 h and subsequent (*1*) quenching and (*2*) slow cooling to 400°C.

The high-coercivity fine phase and domain structures of component A qualitatively differ [11, 12]. Rather, they correspond to the phase and domain structures of quasi-binary $Sm(Co, Cu)_z$ and $Sm(Co, Cu, Fe)_z$ ($z = 5–6$) alloy samples. Upon magnetization reversal, the domain structure transforms from a limited number of centers; this is accompanied by the development of fernlike domains grown isotropically in all directions. In fact, structural component A in cast samples is a model prototype of boundary areas in the typical cellular structure of sintered $(Sm, Zr)(Co, Cu, Fe)_z$ magnets.

The character of the dependences of the coercive force of experimental samples in Figs. 1 and 4b shows that, in samples with a dominating volume fraction of component A which were quenched from the isothermal aging temperature, efficient domain-wall pinning centers are absent; i.e., no phase transformations resulting in the formation of pinning centers in component A in a temperature range from the temperature of solid solution heat treatment to 800°C occur.

In contrast, as a result of stepped aging, highly efficient pinning centers form in structural component A, which ensure the ultimate hysteresis loops of experimental samples. This is likely related to the phase transformations occurring in structural component A in a temperature range of 800–400°C.

The occurrence of phase transformations in structural component A is confirmed by the intense increase in the coercive force of samples with $V_A < V_B$ which were quenched from the isothermal aging temperature.

Diffusion processes in the course of isothermal aging of $(Sm, Zr)(Co, Cu, Fe)_z$ alloys ensure not only the development of cellular phase morphology but also the formation of chemical gradients between structural elements. The processes of redistribution of elements of the alloy between structural components during isothermal heat treatment are not so efficient as those occurring during stepped aging; nevertheless, the processes lead to substantial compositional differences [1, 4, 7, 8]. In particular, the cellular phases of component B (2:17) and component B (as a whole) act as a donor of copper and are enriched in Fe, whereas the boundary phase of component B and structural component A, vice versa, give away Fe and accept Cu.

At the end of isothermal aging, in particular, under conditions of prolonged holding, the main structural components A and B in the (Sm, Zr)(Co, Cu, Fe) samples with $z = 6.0–6.8$ are supersaturated with the corresponding elements to different degrees because of (1) the same level of concentrations of elements in the integral composition of alloy, (2) directional diffusion of elements between structural components that form on the basis of different phases, and (3) wide ranges of variations of volume fractions of A and B in accordance with z of the alloy.

As is known, just copper ensures the formation of pinning centers in the $Sm(Co, Cu)_z$ and $Sm(Co, Cu, Fe)_z$ alloys and in the boundary phase of the $(Sm, Zr)(Co, Cu, Fe)_z$ compositions [7, 8]. It is obvious that the degree of supersaturation of component A in the experimental samples with $V_B > V_A$ reaches values at which the phase transformation ensuring the efficient pinning centers occurs even upon quenching after isothermal annealing. In this case, the higher the volume fraction of component B in the alloy, i.e., the higher the difference $(V_B - V_A)$, the higher the supersaturation of component A with copper and the more efficient the domain-wall pinning centers are after cooling (Fig. 4b, curve *1*).

The above considerations indicate that the variant of phase transformations which assumes the formation of the final phase composition of fine structure of $(Sm, Zr)(Co, Cu, Fe)_z$ alloys upon heat treatment for the high-coercivity state during isothermal aging is untenable.

During isothermal aging of sintered magnets, the solid solution based on the hexagonal 1:7H phase decomposes with the formation of cellular structure. In the samples under study, the structure with the cellular morphology forms within component B. Structural component A is a full analog and continuation of the boundary network going from component B. Therefore, the structure of component A is analogous to the structure of the boundary between cells and is formed by 2:7R and 5:19H phase layers progressively alternating along the *c* axis [6, 7, 9]. In turn, in the course of stepped (or slow) cooling, the final high-coercivity 2:17R + 1:5H structure of the alloy forms owing to element diffusion.

In the (Sm, Zr)(Co, Cu, Fe)$_z$ alloys, which are characterized by a (4*f*-,4*d*-)-to-(3*d*-) element ratio (z) of above a certain value, the dominant volume fraction of structural component B leads to the high supersaturation of component A with copper. This predetermines the occurrence of the 2:7R + 5:19H + Cu $\leftrightarrow$ 1:5H transformation upon quenching without slow (stepped) cooling in a temperature range of 800–400°C. Because of the shortness of quenching process, the phase transformation in component A and at cells boundaries is likely to be incomplete in character. Therefore, the magnetization curves of samples with $V_B > V_A$ quenched after isothermal aging exhibit a worse combination of hysteretic characteristics as compared to that of samples with $V_A \geq V_B$ subjected to slow (stepped) cooling that ensures the completeness of phase transformations. However, taking into account the demagnetizing factor, the equality $4\pi J_S = B_R$ is characteristic also of quenched model samples with high z.

The reversibility of phase transformations easily explains the aforementioned "return" phenomenon for the coercivity force upon short-time heating to the isothermal aging temperature of sintered magnets and model samples prepared from the alloys with low (4*f*-,4*d*-)-to-(3*d*-) element ratios, i.e., with low z indices in the (Sm, Zr)(Co, Cu, Fe)$_z$ formula.

Let us go back to the beginning of the paper. A small comment should be made. The high iron content in the (Sm, Zr)(Co, Cu, Fe)$_z$ alloys and the increase in the relative content of zirconium as well lead to the substantial shift of z, at which the equality of the volume fractions of the main structural components $V_A = V_B$ is reached, to low values of z [11–13].

In the beginning of the paper, specifically, two variants of the composition of sintered samples considered in [1, 7, 9] are given, namely, the original authors' version and that with the separation of 4*f*, 4*d*, and 3*d* elements.

The peculiarities of magnetic hardening of the samples in the course of aging discussed in [1, 7, 9] fit organically into the above considerations. The (4*f*-,4*d*-)-to-(3*d*-) element ratios for the alloys discussed in [1, 7] (z = 5.85 and 5.48, respectively) clearly indicate the fact that the volume fraction of structural component A in the alloys is dominating. Moreover, the composition of samples in [7] is characterized by a relatively high zirconium content. In contrast, for samples with z = 6.6 [9], the fairly high content of structural component B is obvious. This explains the high coercive force of samples [9] subjected to aging at 830°C for 10 h and subsequent quenching.

CONCLUSIONS

(1) Processes of the formation of the high-coercivity state of model samples of (Sm, Zr)(Co, Cu, Fe)z-based alloys of different compositions were systematically studied.

(2) Interrelations between the chemical composition of the samples, their microstructure, coercive force, and magnetic hardening processes occurring in the course of isothermal aging and aging during slow (stepped) cooling were determined.

(3) It was shown that the formation of the high-coercivity state of the $Sm_{0.85}Zr_{0.15}(Co_{0.702}Cu_{0.088}Fe_{0.210})_z$ samples with z = 6.0–6.8 (where z characterizes the (4*f*-,4*d*-)-to-(3*d*-) element ratio) is determined by the ratio of volume fractions of the two main structural components A and B, which integrally correspond to 0.93–0.98 volume fractions.

(4) In the case of the high-coercivity state, the structure of component B is analogous to that of sintered Sm–Zr–Co–Cu–Fe-based magnets and consists of a continuous boundary network formed by phases belonging to the (Sm, Zr)$_{n-1}$(Co, Cu, Fe)$_{5n-1}$ homologous series.

In turn, the structure of component A is analogous to that of boundaries separating cells within structural component B; i.e., the structure is formed on the basis of phases of the (Sm, Zr)$_{n-1}$(Co, Cu, Fe)$_{5n-1}$ homologous series that alternate along the *c* axis, being common for the entire anisotropic body.

(5) The cellular morphology forms in the course of isothermal aging, whereas the final phase composition of component A and boundary network B forms in a temperature range from the isothermal aging temperature to 400°C during stepped (slow) cooling or quenching.

(6) It was found that the magnetic properties of the samples in the high-coercivity state are determined by the completion of phase transformations in component A and boundary network B; this substantially depends on the ratio of volume fractions of the two main structural components A and B and also on the (4*f*-,4*d*-)-to-(3*d*-) element ratio, i.e., the value of z in the (Sm, Zr)(Co, Cu, Fe)$_z$ formula.

FUNDING

This study was supported by the Russian Science Foundation, project no. 20-19-00689.

REFERENCES

1. Sepehri-Amin, H., Thielsch, J., Fischbacher, J., Ohkubo, T., Schrefl, T., Gutfleisch, O., and Hono, K., Correlation of microchemistry of cell boundary phase and interface structure to the coercivity of $Sm(Co_{0.784}Fe_{0.100}Cu_{0.088}Zr_{0.028})_{7.19}$ sintered magnets, *Acta Mater.*, 2017, vol. 126, pp. 1–10.
2. Gopalan, R., Ohkubo, T., and Hono, K., Identification of the cell boundary phase in the isothermally aged commercial $Sm(Co_{0.725}Fe_{0.1}Cu_{0.12}Zr_{0.04})_{7.4}$ sintered magnet, *Scripta Mater.*, 2006, vol. 54, pp. 1345–1349.
3. Fidler, J., Bernardi, J., and Skalicky, P., Analytical electron microscope study of high- and low-coercivity SmCo 2:17 magnets, *Mater. Res. Soc. Symp. Proc.*, 1987, vol. 96, pp. 181–192.
4. Ray, A.E., A revised model for the metallurgical behavior of 2:17-type permanent magnet alloys, *J. Appl. Phys.*, 1990, vol. 67, no. 9, pp. 4972–4074.
5. Delannay, F., Derkaoui, S., and Allibert, C.H., The influence of zirconium on $Sm(CoFeCuZr)_{7.2}$ alloys for permanent magnets I: Identification of the phases by transmission electron microscopy, *J. Less Common Met.*, 1987, vol. 134, pp. 249–262.
6. Derkaoui, S., Allibert, C.H., Delannay, F., and Laforest, J., The Influence of zirconium on $Sm(Co, Fe, Cu, Zr)_{7.2}$ alloys for permanent magnets II: Composition and lattice constants of the phases in heat-treated materials, *J. Less Common Met.*, 1987, vol. 136, pp. 75–86.
7. Goll, D., Kronmüller, H., and Stadelmaier, H.H., Micromagnetism and the microstructure of high-temperature permanent magnets, *J. Appl. Phys.*, 2004, vol. 96, pp. 6534–6545.
8. Zhang, Y., Tang, W., Hadjipanayis, G., Chen, C., Nelson, C., and Krishnan, K., Evolution of microstructure, microchemistry and coercivity in 2:17 type Sm-Co magnets with heat treatment, *IEEE Trans. Magn.*, 2001, vol. 37, pp. 2525–2527.
9. Song, K., Fang, Y., Wang, S., Yu, N., Chen, H., Zhang, M., Zhu, M., and Li, W., Crystalline and magnetic microstructures of iron-rich $Sm(Co_{0.65}Fe_{0.26}Cu_{0.07}Zr_{0.02})_{7.8}$ sintered magnets: Isothermal aging effect, *J. Magn. Magn. Mater.*, 2018, vol. 465, pp. 569–577.
10. Burkhanov, G.S., Dormidontov, N.A., Kolchugina, N.B., and Dormidontov, A.G., Effect of sintering in a hydrogen atmosphere on the density and coercivity of (Sm, Zr) (Co, Cu, Fe)$_z$ permanent magnets, *IOP Conf. Ser.: Mater. Sci. Eng.*, 2018, vol. 347, art. ID 012023.
11. Suponev, N.P., Shamorikova, E.B., Dormidontov, A.G., Titov, Yu.V., Lukin, A.A., and Levandovskii, V.V., *Struktura i magnitnye svoystva splavov Sm–Zr–Co–Cu–Fe v vysokokoertsitivnom sostoyanii. 1. Strukturnye sostavlyayushchie i protsessy peremagnichivaniya. Fizika magnitnykh materialov* (Structure and Magnetic Properties of Sm–Zr–Co–Cu–Fe Alloys in a Highly Coercive State. 1. Structural Components and Processes of Magnetization Reversal. Physics of Magnetic Materials), Kalinin: Kalinin. Univ., 1988, pp. 93–106.
12. Suponev, N.P., Dormidontov, A.G., Levandovskii, V.V., Shamorikova, E.B., and Nekrasova, E.M., *Struktura i magnitnye svoystva splavov Sm–Zr–Co–Cu–Fe v vysokokoertsitivnom sostoyanii. 2. Model' formirovaniya struktury. Fizika magnitnykh materialov* (Structure and Magnetic Properties of Sm–Zr–Co–Cu–Fe Alloys in a Highly Coercive State. 2. Model of Structure Formation. Physics of Magnetic Materials), Tver: Tver. Univ., 1992, pp. 78–98.
13. Dormidontov, A.G., Kolchugina, N.B., Dormidontov, N.A., and Milov, Y.V., Structure of alloys for (Sm, Zr)(Co, Cu, Fe)$_z$ permanent magnets: First level of heterogeneity, *Materials*, 2020, vol. 13, no. 17, art. ID 3893.

Translated by N. Kolchugina